ACCIDENT SIMULATIONS OF A NOVEL RESTRAINT SAFETY CONCEPT FOR MOTORCYCLISTS

Steffen Maier, Jörg Fehr
Institute of Engineering and Computational Mechanics, University of Stuttgart
Germany

Paper Number 23-0189

ABSTRACT

Except for personal protective equipment, riders of powered two-wheelers are currently unprotected when impacting into an accident opponent. This work investigates a motorcycle safety concept that proposes a combination of thigh seat belts, airbags, and leg impact protectors. It gives a virtual prediction of the accident behavior using finite element models of the motorcycle with passive safety systems, an accident opponent, and an anthropometric test device as a rider surrogate in recommended frequent accident scenarios. It shows a meaningful graphical description of the functional and causal principles of a powered two-wheeler rider restraint and a quantified performance evaluation of the concept. The combination of several passive safety systems has shown to be promising in positively influencing accident behavior and mitigating consequences.

INTRODUCTION

From economic and environmental perspectives, powered two-wheelers (PTWs) are an efficient mode of transportation. Because of high traffic volume, many cities have already reached their capacity limits at peak traffic times. A shift to smaller vehicles can provide much-needed relief. A case study of the Leuven-Brussels motorway journey [1] examines the impact of a modal shift in which 10 % of cars are replaced by PTWs. The traffic flow model simulation states that traffic loss hours decrease by 63 % from 1925 hours in a reference scenario to only 706 hours lost. Also, regardless of the type of drive, PTWs consume fewer resources in production and have a lower energy consumption and use less space than cars. Considering the average occupancy (e-scooter: 1.1 persons vs., e.g., a mid class passenger car: 1.34 persons) in an evaluation of different transportation modes for urban areas [2], e-scooters perform among the best regarding the energy demand in use. They are more efficient than other electric vehicles, buses, and the tram; only bicycles and e-bicycles are more efficient than electric PTWs. However, their poor passive safety is their decisive disadvantage at considerable social costs.

A comparison of the fatality risks of various modes of transportation (cars & light trucks, pedestrians & bicycles, motorcycles, large trucks, buses, maritime, aviation, railroads, pipeline) in the US for 2000-2009 [3] shows that riding a motorcycle is by far the most dangerous. Riding a motorcycle accounts for 212 fatalities per billion passenger miles; driving or being a passenger in a car or light truck only accounts for 7.28 fatalities per billion miles traveled. This is because motorcycles do not provide anywhere near the same level of crashworthiness and rider protection as automobiles do for their occupants. A car is much more stable and easier to see. In the event of an accident, a car has the advantage of significantly more weight and volume. It fully encloses the occupants in a safety cell and provides passive safety features such as seat belts and airbags. In contrast, the safety equipment of most motorcyclists is currently limited to personal-worn protective equipment. The current safety strategy of conventional motorcycles does not go beyond the intention or, even more so, hope that the vehicle user will be able to get as little as possible entangled with the motorcycle and will be thrown off quickly instead.

There are two main approaches to passive safety in motorcycle literature [4]. In the first principle, the rider is restraint to the motorcycle. In a collision, kinetic energy from the motorcycle is converted into

deformation work. The rider restraints, e.g., belts or airbags, aim to prevent direct contact between the motorcyclist and an accident opponent up to a certain collision speed. Production motorcycles that aim for that principle are rare. The Honda Goldwing is a large tourer equipped with a frontal airbag [5, 6, 7]. The BMW C1 is a city scooter with a rollover structure and belt restraint for an upright seated rider [8, 9].

In the second principle, the rider must be separated from the motorcycle as soon as possible, and a direct impact must be avoided. Here, the rider mustn't get tangled up in parts of the motorcycle. In the best case, a flyover of the motorcyclist over the accident opponent is initiated. The principle aims that the injuries of a flyover should be less than those of a direct impact. Most motorcycles aim for this safety principle. Several types of rider kinematics have been identified for impacts with these conventional motorcycles, see e.g. [10, 11], for experiments including a pillion passenger [12]. The observed patterns can be divided, as shown by [13], into one of the types illustrated in Figure 1: (a) a direct impact, (b) a rollover, or (c) a flyover of the rider. Before impact, this depends on the points of contact at the collision opponents; during the collision phase, it depends on the vehicle geometries and the structural properties. In a direct impact, the rider is decelerated the most; hence the resulting immediate energy input into the rider is the highest. For a rollover, the energy input is lower, and for a flyover even lower. In the case of a rollover or flyover, the rider detaches from the motorcycle, which remains the decisive safety principle of today's motorized two-wheelers. This assumes that injuries in the subsequent so-called secondary accident phase will be less than in a direct car impact. The chances of being injured less severely or not at all are promising only if the rider is wearing effective personal protective equipment and slides freely to the final position after impact without coming into contact with other vehicles or fixed objects.

(a) direct impact
high energy transfer

(b) rollover with
medium energy transfer

(c) flyover with
low energy transfer

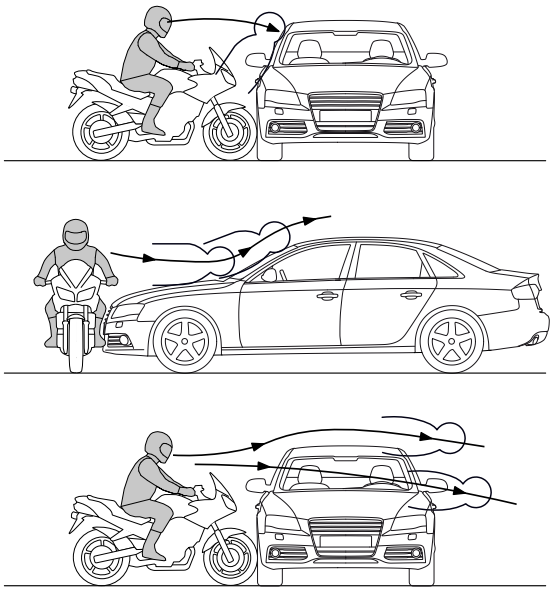

Figure 1: **Types of collisions of a conventional motorcycle and rider against an opposing vehicle.**

The safe motorcycle studied here aims at the first principle. It consists of a newly designed motorcycle frame and body, seat belts, multiple airbags, foam leg impact protectors, and a side impact structure; see full FE model in Figure 2. The concept, initially described in [14], envisages that in the event of an impact, the two belts around the thighs restrain the rider to the motorcycle. The surrounding airbags then decelerate the upper body rotation in a controlled manner and protect the rider from hard contact with an opposing vehicle, the road, or road-side structures. The foam impact protectors absorb the impact of the legs on the motorcycle cockpit and the side impact structure protects the lower extremities laterally. The concept's idea is to preserve the open design and superior all-around visibility and maneuverability of a two-wheeler without any rollover structure. The goal is to supersede a motorcycle rider's safety clothing and helmet entirely in the future and, therefore, significantly increase the suitability of motorcycles as commuter vehicles and/or shared mobility solutions.

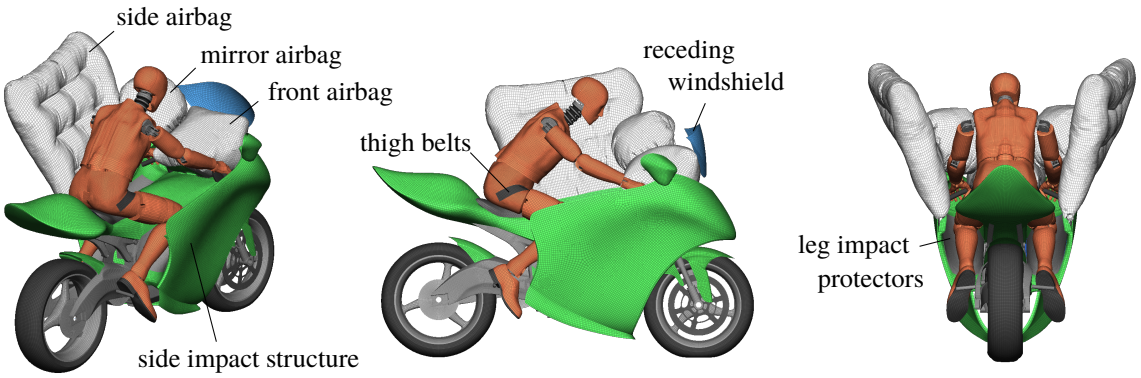

Figure 2: **FE motorcycle with restraint safety concept and Hybrid III 50th ATD as rider surrogate.**

This paper presents the tools and methods to design an optimal and robust novel safety concept for motorcycles. The safety concept combines well-established safety strategies of occupant protection onto a motorcycle to minimize the intrinsic unpredictability of PTW crashes. The novelty of this work is the investigation of the PTW safety concept in a full FE approach, as part of a modeling and simulation strategy with different levels of model fidelity. It aims for a meaningful description of the operating principles and their influence on the accident behavior in comparison to a conventional PTW based on the virtual models.

MODELING

The work presented here is part of a a multi-stage, multi-model approach with varying degrees of model fidelity, outlined in Figure 3.

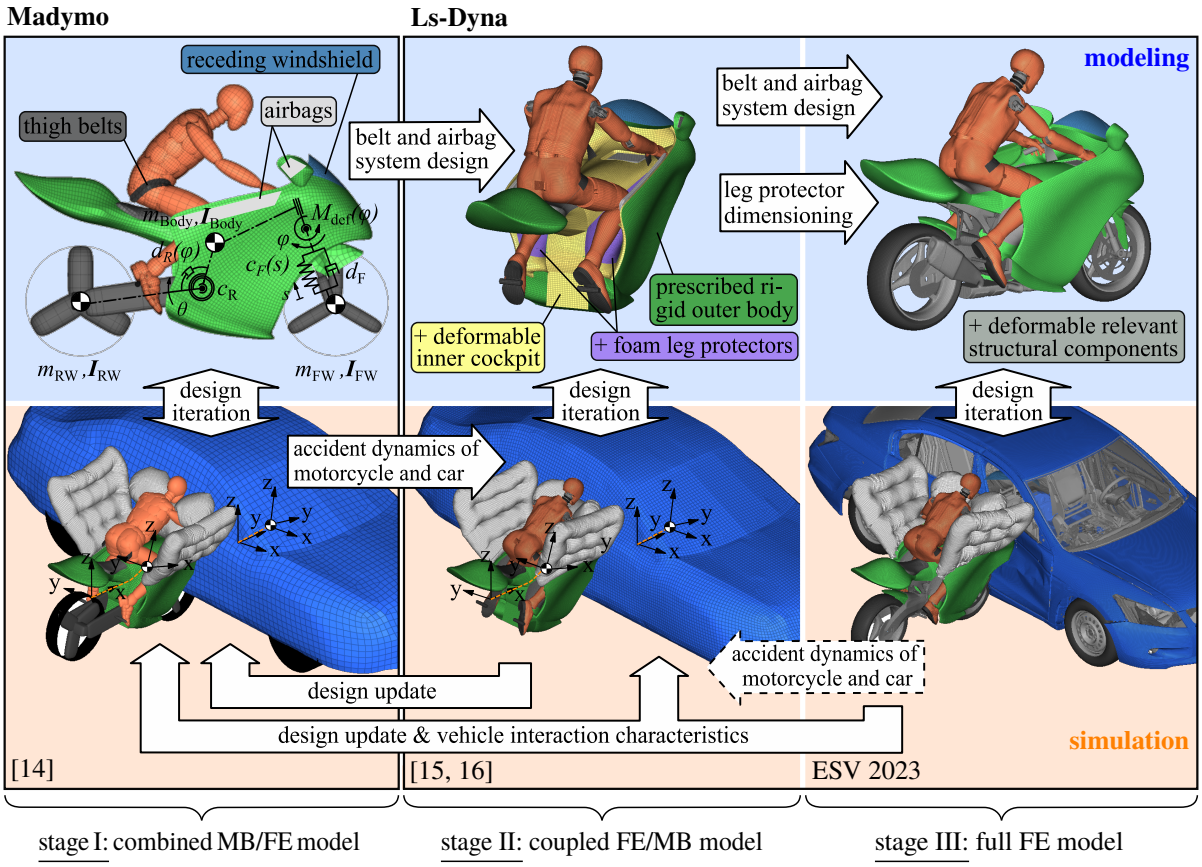

Figure 3: **Modeling and simulation strategy.**

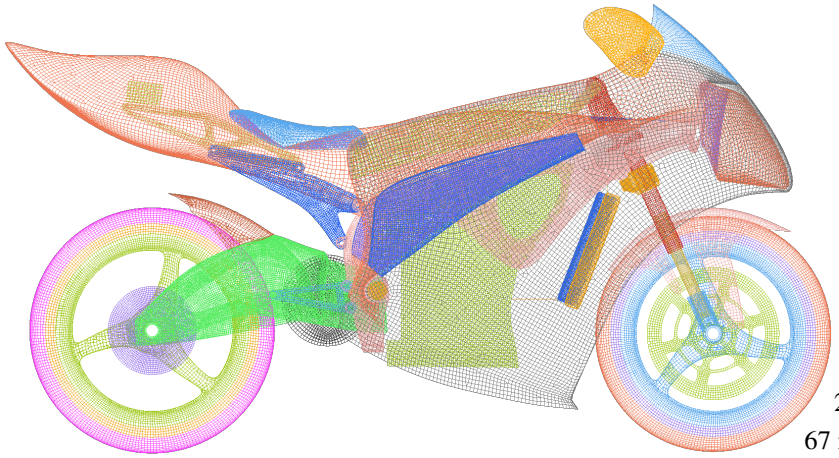

81 parts
323,000 nodes
60 beam elements
243,000 shell elements
135,000 solid elements

12 joint connections
25 extra node set connections
67 nodal rigid body connections

Figure 4: **Discretization of the FE motorcycle model, shown as wireframe elements.**

The modeling and simulation strategy consists of three stages (I) to (III): (I) In the MADYMO software environment[1], the motorcycle, airbags, belts, rider surrogate, and accident opponent are modeled in a combined multibody and FE approach, introduced in [14]. Vehicle deformation and contact characteristics, as well as an effectiveness assessment of the passive safety systems are based on fitted simulation models of full-scale crash tests of conventional motorcycles. (II) An equivalent FE model of the rider interaction surfaces, coupled to accident trajectories from MB simulations, includes the leg impact protectors in the LS-DYNA software environment[2], introduced in [15, 16] also used in [17]. (III) Simulations of a full FE approach in LS-DYNA that also includes the motorcycle's structurally relevant components as deformable parts.

In this work, the proposed motorcycle is investigated in the shown full FE model approach (stage III), shown in Figure 4.

The model aims to represent the interaction with the crash opponent, structural loading and deformation, and energy absorption of the motorcycle structure. As a result, its focus is on representing the crash-relevant structural components, which are the front wheel, front tire, and front suspension assembly. Components such as the drivetrain are modeled as rigid parts because they are assumed not to deform because they are very stiff or outside of the crash deformation. As a unique feature of the proposed motorcycle structure a foam crash box in the cockpit nose aims to control the energy transfer. This prevents a rollover in a frontal impact. The elevated side impact structures protect the lower extremities laterally. In total, the model consists of 81 parts from 378,000 elements with 323,000 nodes. The suspension is modeled with eight kinematic joints; front wheel rotation (2), telescopic front fork suspension (2), rear-wheel rotation (2), front fork steering, and rear swing arm rotation. The other kinematic joints are for the lids of the compartments behind which the airbags are located.

Recent other detailed FE models of PTWs for crash investigations are [7] (a large tourer), [18] (a three-wheeled scooter), [19] (a sport bike), and [20] (a sport tourer).

[1]SIEMENS Simcenter Madymo (version 2021.1 SMP): `https://www.plm.automation.siemens.com/global/en/products/simcenter/madymo.html`

[2]Ansys LS-DYNA (version R9.3.1 MPP): `https://www.ansys.com/products/structures/ansys-ls-dyna`

Impact configurations

As a set of representative impact scenarios, accident configurations from ISO1323 [21] are used. The standard isolates seven representative impact configurations ① to ⑦, shown in Figure 5. The set includes collisions between a motorcycle and a passenger car, with the motorcycle and car, either stationary or moving forward up to a speed of ≈48 km/h (13.4 m/s). The contact points on the motorcycle and car are at the front and side, respectively. There are no rear contacts included (either at the car or at motorcycle). The standard defines the opposing vehicle as a four-door saloon with a mass of 1,238-1,450 kg and an overall height of 137-147 cm. The set does not include scenarios with roadside barriers. As the accident opponent, the FE model of a 2001 Ford Taurus [22] is used. The model, developed and validated by the National Crash Analysis Center (NCAC), is publicly available in the NHTSA vehicle database [23]. With an overall height of 147 cm and a mass of 1477 kg the four-door passenger sedan complies with [24] specifications for the opposing vehicle height but slightly exceeds vehicle mass.

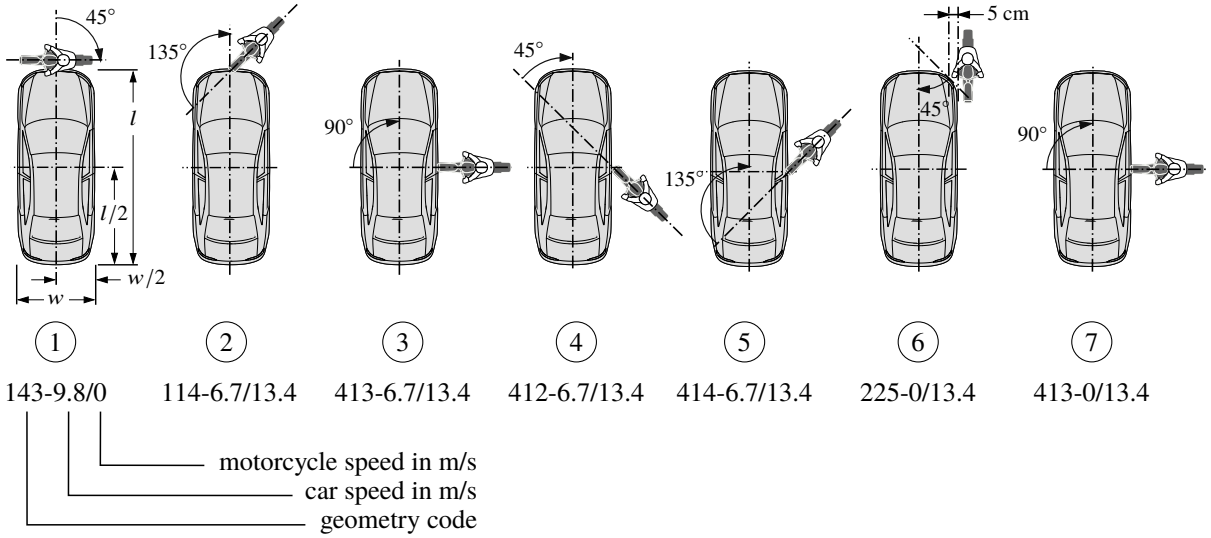

Figure 5: **Representative set of impact configurations according to [21].**

Injury criteria

For passenger vehicle occupant protection, there are national and international regulations, such as the ECE regulations by the United Nations Economic Commission for Europe (UNECE) or Federal Motor Vehicle Safety Standards (FMVSS) for the US that specifies injury criteria and respective maximal values for specific load cases. Also, consumer ratings such as the New Car Assessment Programs for the United States (US NCAP) and the European Union (Euro NCAP) provide constantly updated biomechanical criteria from the latest scientific findings of occupant protection. To the best of the authors' knowledge, for the passive safety of motorcyclists, such governmental regulations or consumer ratings currently do not exist. The most recent version of ISO 13232 recommends only a very limited set of criteria. The work presented here aims to assess many potential injury mechanisms for the whole body. The selection of injury criteria considered are summarized in Table 1. It is based on a comprehensive set of injury criteria and corresponding biomechanical limits for motorcyclists from an extensive literature review by [25]. This selection is extended to include the GAMBIT, which is recommended in the international standard [26], as well as the BrIC and the Nij criterium. For femur criteria, stricter thresholds from ECE-R 94 [27] are used.

body region	injury criterion		limit (Hyb III 50th)	ref.
head	resultant acceleration	$a_{t_{\text{int}}} = \max_{t_1}\left(\min_{t_1 \le t \le t_1 + t_{\text{int}}} a_{\text{res}}(t)\right)$	80 g for t_{int} = 3 ms	[27]
	head injury criterion	$\text{HIC}(t_2 - t_1) = \max_{t_1, t_2}\left\{(t_2 - t_1)\left[\frac{1}{t_2 - t_1}\int_{t_1}^{t_2} a_{\text{res}}(t)dt\right]^{2.5}\right\}$ with $a_{\text{res}}(t)$ in g and t in s	1000 for $t_2 - t_1 \le 36$ ms	[28, 29]
	generalized acceleration model for brain injury threshold	$\text{GAMBIT} = \left[\left(\frac{a_{\text{res}}(t)}{a_{\text{C}}}\right)^{2.5} + \left(\frac{\ddot{\varphi}_{\text{res}}(t)}{\ddot{\varphi}_{\text{C}}}\right)^{2.5}\right]^{\frac{1}{2.5}}$ with a_{C} = 250 g and $\ddot{\varphi}_{\text{C}}$ = 25 krad/s^2	1	[30]
	brain injury criterion	$\text{BrIC(CSDM)} = \sqrt{\left(\frac{\max\lvert\omega_x(t)\rvert}{\omega_{xC}}\right)^2 + \left(\frac{\max\lvert\omega_y(t)\rvert}{\omega_{yC}}\right)^2 + \left(\frac{\max\lvert\omega_z(t)\rvert}{\omega_{zC}}\right)^2}$ with $\omega_{xC} = 66.2, \omega_{yC} = 59.1, \omega_{zC} = 44.25$ rad/s	1	[31]
neck	tensile force	$F_{z,\text{tens},t_{\text{int}}} = \max_{t_1}\left(\min_{t_1 \le t \le t_1 + t_{\text{int}}} F_z(t)\right)$	3.3 kN for t_{int} = 1 ms 1.1 kN for t_{int} = 45 ms	[32, 29]
	compression force	$F_{z,\text{compr},t_{\text{int}}} = \min_{t_1}\left(\min_{t_1 \le t \le t_1 + t_{\text{int}}} F_z(t)\right)$	4 kN for t_{int} = 1 ms 1.1 kN for t_{int} = 45 ms	
	shear force	$F_{xy,t_{\text{int}}} = \max_{t_1}\left(\min_{t_1 \le t \le t_1 + t_{\text{int}}} \sqrt{F_x(t)^2 + F_y(t)^2}\right)$	3.1 kN for t_{int} = 1 ms 1.1 kN for t_{int} = 45 ms	
	forward moment	$M_{y,\text{fwd,max}} = \min M_y(t)$	190 Nm	
	rearward moment	$M_{y,\text{rwd,max}} = \max M_y(t)$	57 Nm	
	neck injury criterion	$\text{Nij}_{\text{max}} = \max\left(\left\lvert\frac{F_z(t)}{F_{\text{int}}}\right\rvert + \left\lvert\frac{M_y(t)}{M_{\text{int}}}\right\rvert\right)$ with $F_{\text{int,C/T}} = 6160/6806$ N, $M_{\text{int,F/E}} = 310/135$ Nm	1	[28, 33, 29]
thorax	resultant acceleration	$a_{t_{\text{int}}} = \max_{t_1}\left(\min_{t_1 \le t \le t_1 + t_{\text{int}}} a_{\text{res}}(t)\right)$	60 g for t_{int} = 3 ms	[29]
	thorax compression	$\text{ThCC} = \max s(t)$	50 mm	[27]
	viscous criterion	$\text{VC}_{\text{max}} = \max(\text{V}(t) \cdot \text{C}(t))$	1 m/s	[34, 27]
pelvis	resultant acceleration	$a_{t_{\text{int}}} = \max_{t_1}\left(\min_{t_1 \le t \le t_1 + t_{\text{int}}} a_{\text{res}}(t)\right)$	60 g for t_{int} = 3 ms	[25]
femur	axial force	$\lvert F_z\rvert_{\text{max}} = \max\lvert F_z(t)\rvert$	9.07 kN	[27]
tibia	tibia index	$\text{TI}_{\text{max}} = \max\left(\left\lvert\frac{\sqrt{M_x(t)^2 + M_y(t)^2}}{(M_{\text{C}})_{\text{res}}}\right\rvert + \left\lvert\frac{F_z(t)}{(F_{\text{C}})_z}\right\rvert\right)$ with $(M_{\text{C}})_{\text{res}} = 225$ Nm and $(F_{\text{C}})_z = 35.9$ kN	1.3	[35, 27]

Table 1: **Selected injury criteria with biomechanical limits for the Hybrid III 50th ATD.**

ACCIDENT SIMULATION

Conventional Motorcycle

For comparison, a full laboratory crash test of a conventional motorcycle against a passenger car is used. It is an impact according to ISO 12323 (7) with a helmeted Hybrid III 50th anthropometric test device (ATD) as part of investigations of [25], to which data we have access to. The laboratory tests are documented with a test protocol and high-speed video footage, a 15-channel sensor data set of the ATD, and accelerometers at multiple points on the motorcycle. The test is then simulated with the MBS approach, see [14], shown in Figure 6.

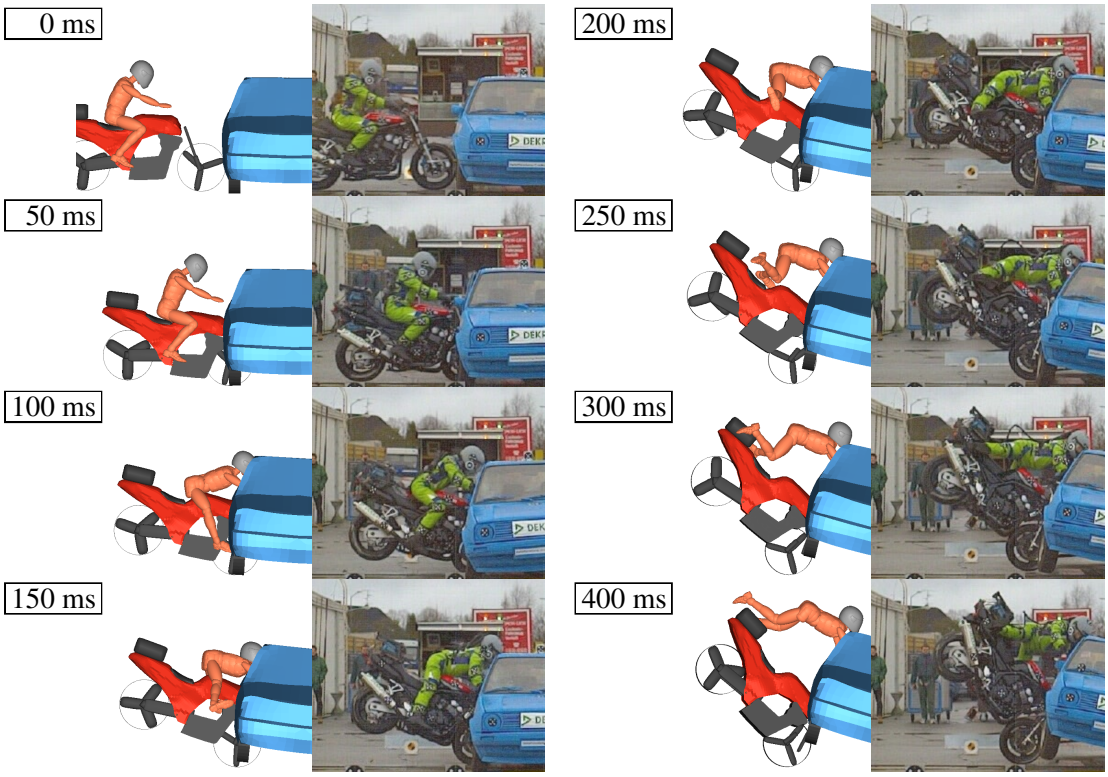

Figure 6: **MB simulation (stage I) of full-scale crash test SH01.01 [25] of a conventional motorcycle Yamaha FZS 600 Fazer and a helmeted Hybrid III 50th against a VW Golf II in scenario (7).**

Figure 7 illustrates the resulting deceleration from the MB simulation of the motorcycle, the opposing vehicle, and the main body parts of the rider for the conventional motorcycle impact by plotting the velocities. The velocities are filtered with a CFC (channel frequency class) filter, see [36]. The impact causes the motorcycle to decelerate relatively uniformly from the initial speed, initiating a forward rotation of the PTW. After the rider is not decelerated until about 40 ms, he is abruptly decelerated by the impact of the pelvis on the tank and the helmeted head on the car. According to the classification in Figure 1, the collision corresponds to a direct impact with a high energy transfer.

A classification into accident phases in Figure 8 reduces the accident occurrence to a chronology of significant events. It illustrates long dead times of the rider's head, pelvis, and legs. Tank impact and helmeted car impact are concentrated short-time events. These lead, i.a., to a high deceleration of the head ($a_{3\text{ms}}$), a very high neck axial compression ($F_{z,\text{compr},1\text{ms}}$) and shear loading ($F_{xy45\text{ms}}$), and a high rearward (extension) moment ($M_{y,\text{rwd,max}}$), see the evaluation of the injuria criteria in Figure 15. The greyed fields ("N/A") are injury criteria that could not be determined with the ATD sensor channels of SH 01.01.

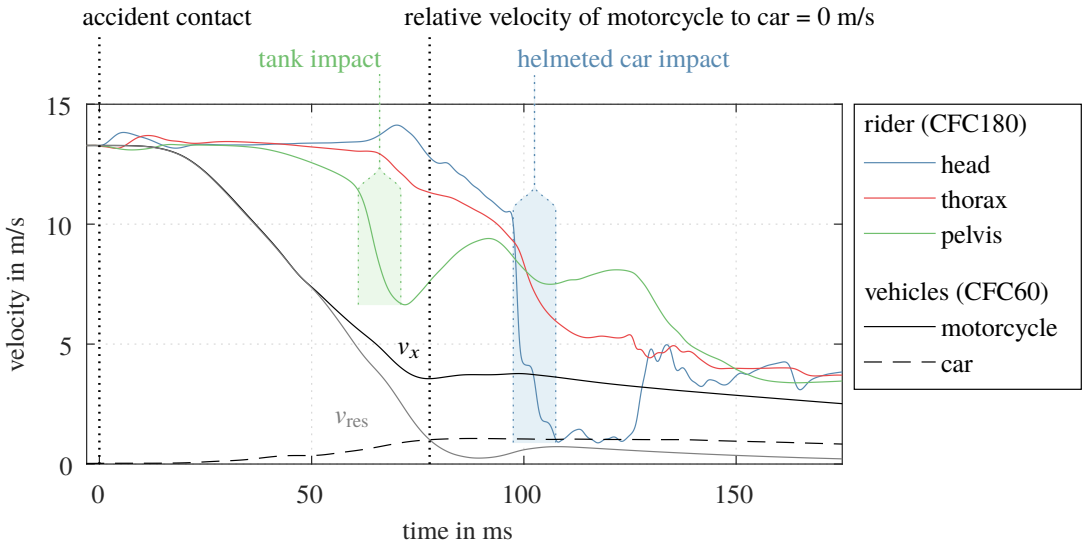

Figure 7: **Velocities of conventional motorcycle and motorcyclist's main body parts relative to car's velocity in a frontal collision according to scenario ⑦ (MB simulation shown in Figure 6).**

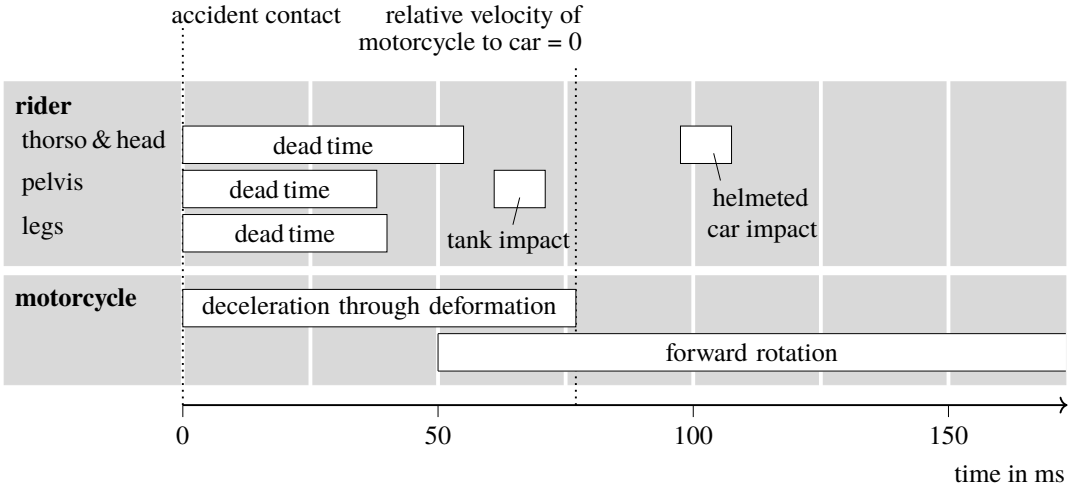

Figure 8: **Schematic chronology of conventional motorcycle and rider behaviour in a frontal collision according to configuration ⑦ (MB simulation of Figure 6).**

Motorcycle with Restraint System

To analyze the safe motorcycle with rider restraint, all seven ISO 13232 scenarios are simulated using the full FE model; see overview in Figure 9. It shows the accident kinematics up to 500 ms each, referred to as the primary impact phase. For the impacts shown, the effect of the safety system can be summarized as follows: The belts restrain the rider to the motorcycle, with the belt load-limiting devices limiting the pelvis accelerations. The belt restraint establishes a pivot point at the pelvis to guide the upper body in forward and sideward rotations and to keep the riders' bodies within the range of the airbags and within the leg protectors and side-impact protection structure. The surrounding airbags decelerate the upper body motion and prevent impact against hard structures, such as the uncushioned motorcycle cockpit surfaces and the accident opponent. The motorcycle cockpit and the accident opponent are reaction surfaces for the airbags.

solver run times:

59.9 h/16 CPUs/MPP/single precision/Ls-DYNA R9.3.1

with AMD Ryzen 9 5950X 16-Core CPU@3.4GHz

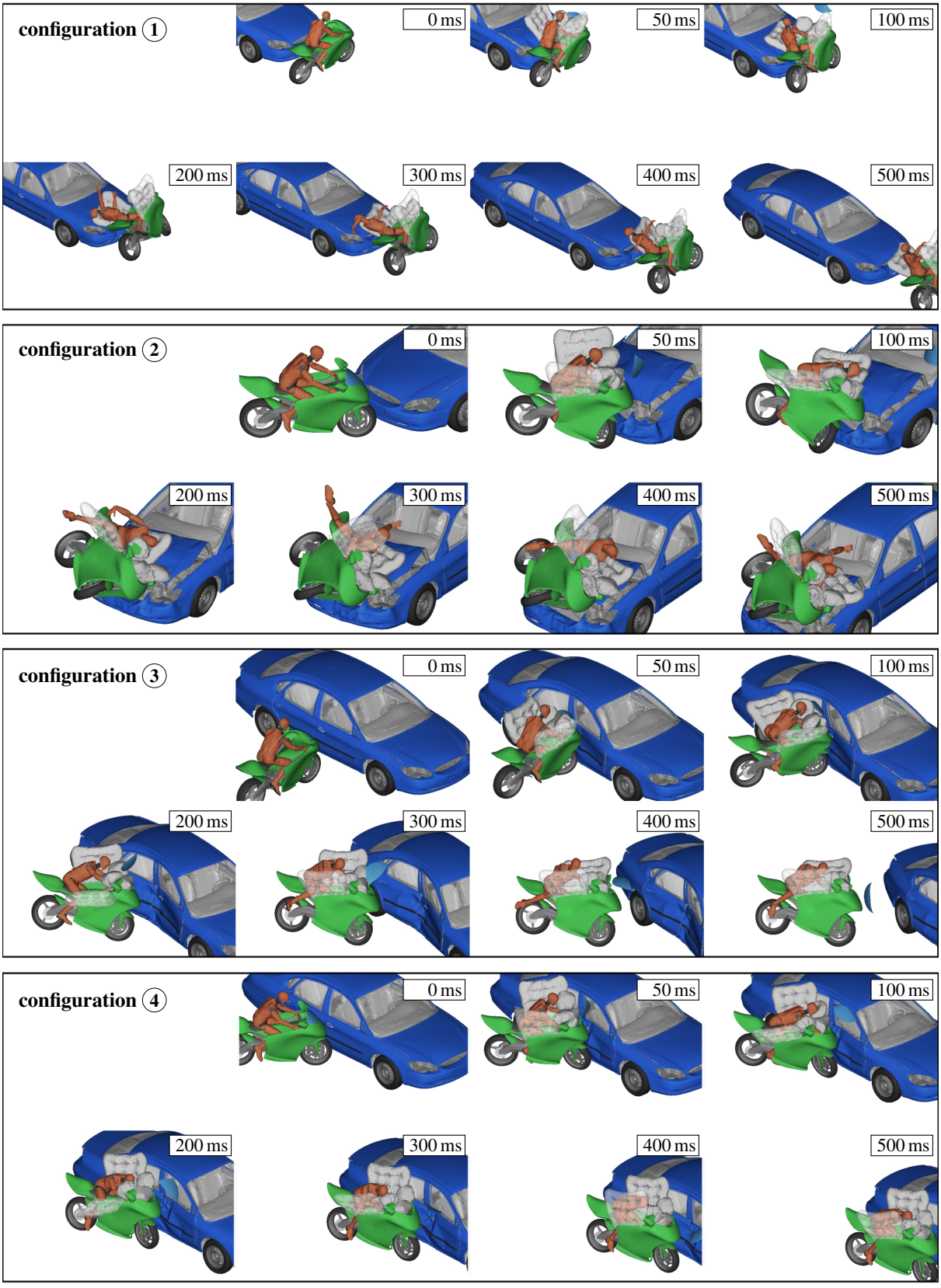

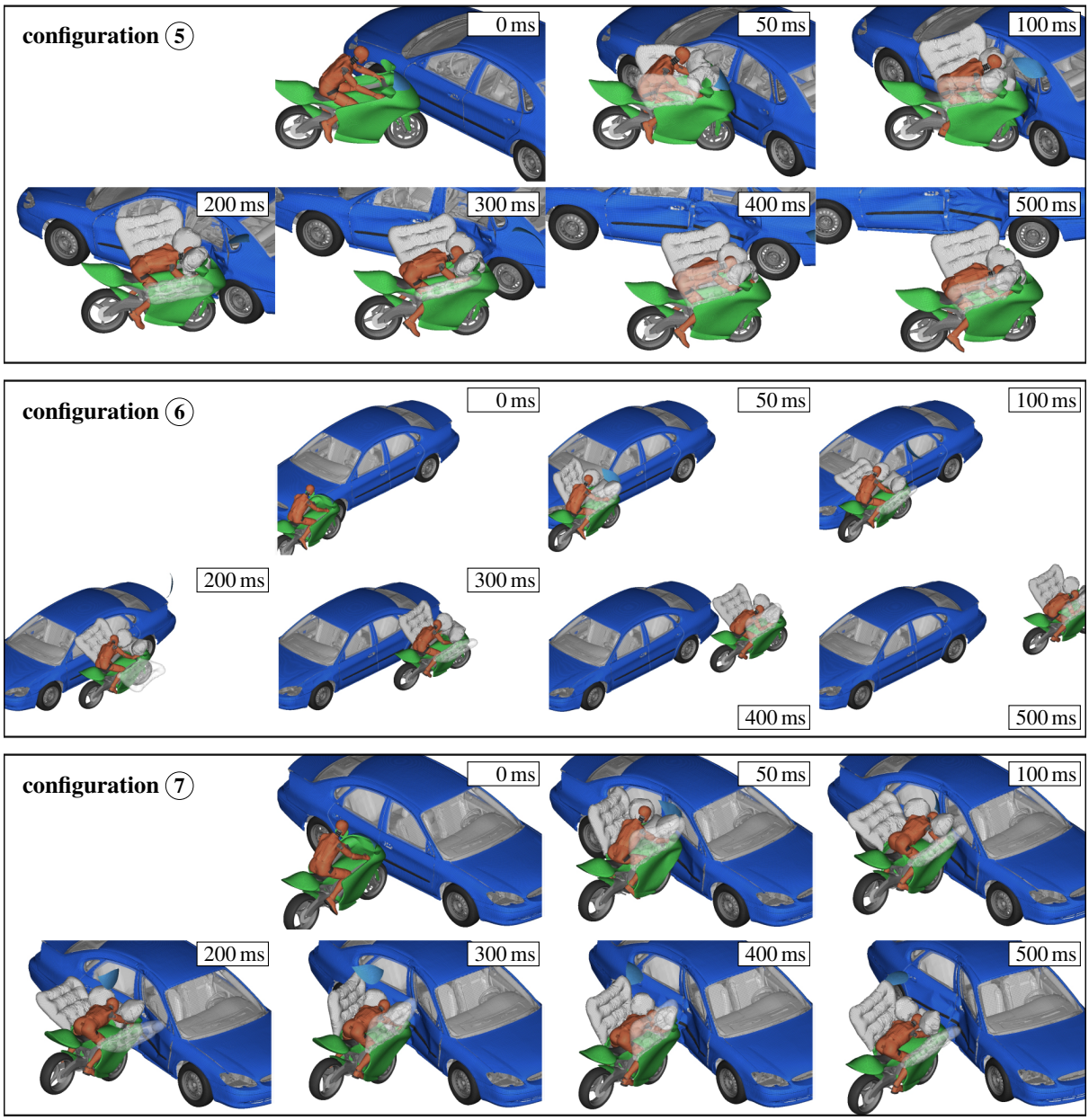

Figure 9: **Primary impact response of motorcycle with restraint system in full FE simulations of ISO 13232 configurations with a non-helmeted Hyb III 50th up to 500 ms.**

Scenarios ① – ③, ⑤, and ⑦ are impacts where the motorcycle is particularly violently de- or accelerated. In scenario ④, the motorcycle bounces off at a shallow angle without losing much speed. In near miss scenario ⑥, the motorcycle grazes the car. The latter two scenarios are particulary interesting for analyzing the secondary accident behavior because much residual energy remains in the motorcycle and the passenger. This also applies to scenarios ① and ② because the car accelerates the motorcycle through the collision.

The heat map in Figure 10 illustrates an evaluation of the biomechanical injury criteria. The selected criteria from Table 1 are normalized to their respective biomechanical limit for the Hybrid III 50th ATD and are color-coded to indicate the severity of the body loads. Overall, only the tibia index (TI) from tibia forces and moments, the brain injury criterion (BrIC) based on head angular velocity, and the thorax acceleration $a_{3\text{ms}}$ criterion exceed their biomechanical limits in some scenarios. Simulations of the safety

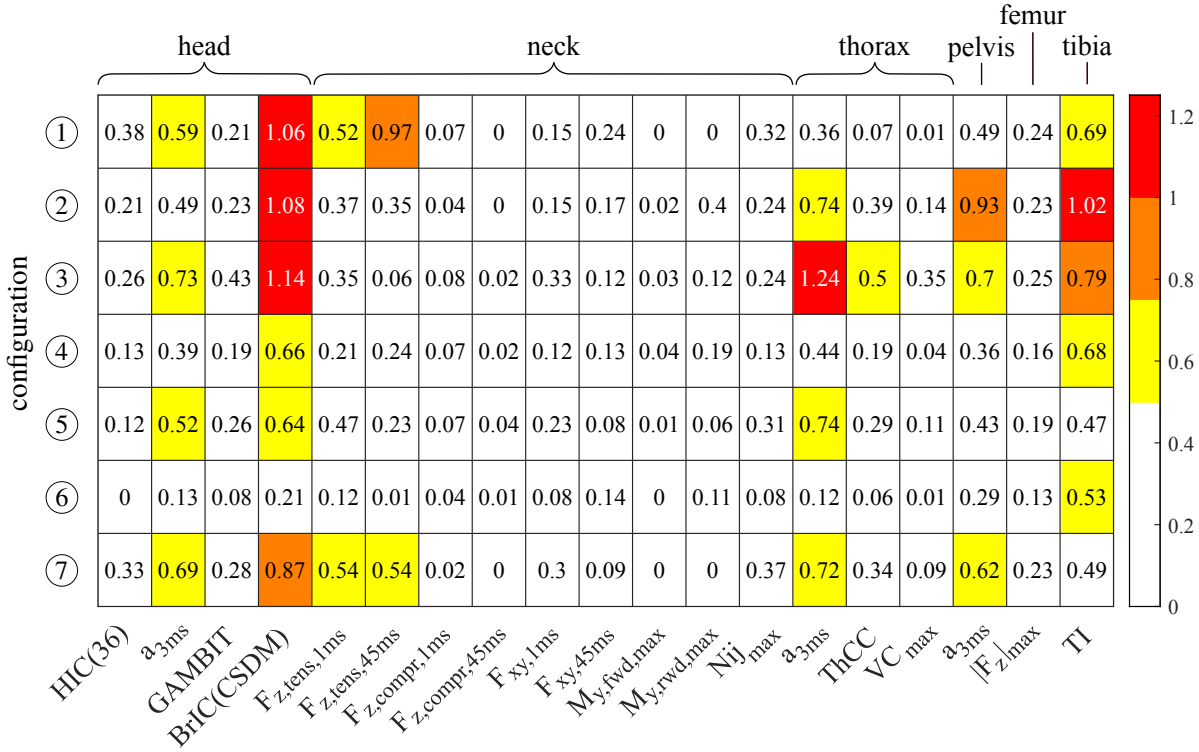

Figure 10: **Injury criteria relative to biomechanical limits for primary impact up to 500 ms shown in Figure 9.**

concept with HBMs [17] also show high BrIC values, exceeding the recommended threshold. The high thorax a_{3ms} values in ③ are due to the arms getting caught in the cockpit fairing and being mechanically locked which transmits a shock trough the rigid arm joints into the torso. Apart from these, the highest values are the head and pelvis a_{3ms} acceleration and neck axial tension. These are concept-related mainly dependent on the belt restraint's load limit, which is a tradeoff between the feasible frontal displacement of the rider and tolerable body loads. A lower belt load limit reduces body loads from the rider restraint but also increases the risk of the head hitting the accident opponent. The leg protectors and side impact protection keep femur axial loading low.

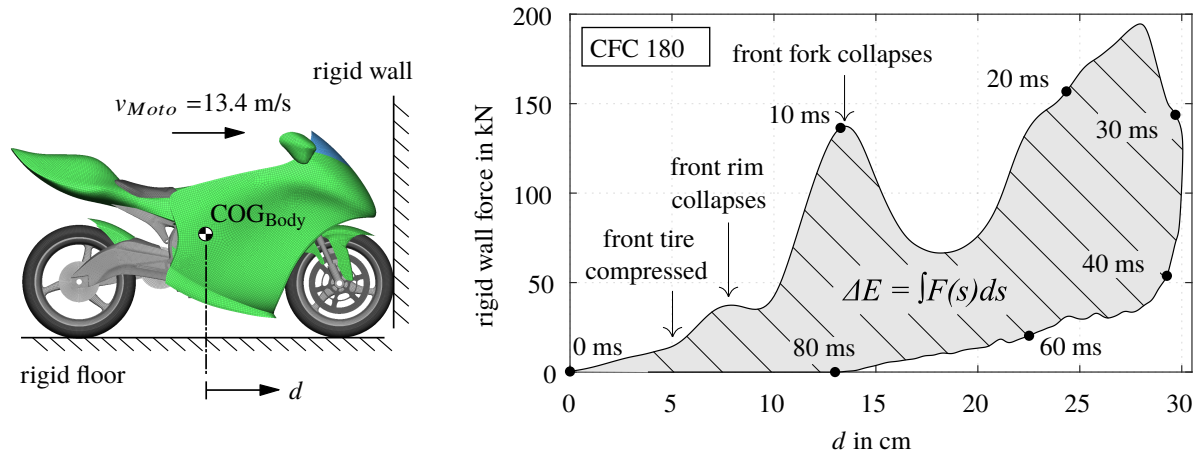

Figure 11: **Frontal deformation characteristics of motorcycle.**

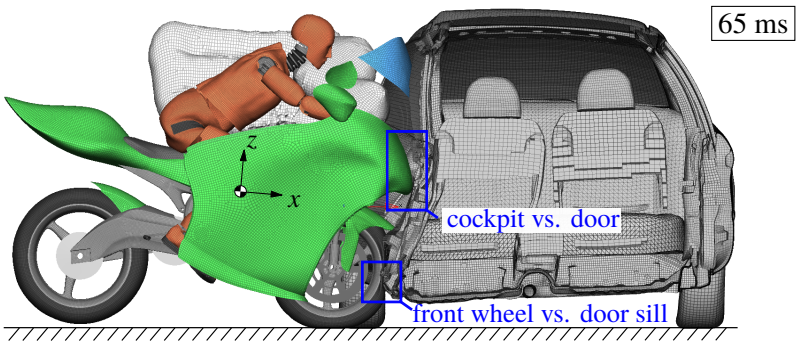

Figure 12: **Motorcycle to car structural interaction and intrusion behaviour in full FE simulation (right airbags are not displayed).**

Unlike the conventional motorcycle collision, the proposed motorcycle does not roll over about its transverse axis during a frontal impact. The voluminous cockpit and the resulting high contact point prevent pitching. Figure 11 illustrates the designed frontal deformation characteristics in impact with a rigid wall. It identifies subsequent phases of deformation: (i) compression of the front tire, (ii) collapse of the front rim, and (iii) collapse of the front fork. The area enclosed corresponds to the dissipated energy. Figure 12 reveals the structural interaction and intrusion of the motorcycle against the opposing vehicle. The motorcycle's front wheel collides with the sill of the car, and the motorcycle cockpit deforms the car door inward.

Figure 13 shows equivalent to Figure 7 the deceleration based on the velocities of the motorcycle and the main body parts of the rider in a frontal collision (scenario ⑦). It shows quite descriptive the benefits of the safety system concept. The belts interact early leading to a relatively continuous deceleration by restraining the pelvis. After about 80 ms, the front airbag decelerates the upper body rotation. Overall the main body parts are decelerated continuously over an increased time period, compared to the short-term impacts of the conventional motorcycle. Plotting a schematic chronology results in Figure 14. Extended by a safety systems layer, it shows the timing and operating phases of the seat belt and airbag systems as well as the leg impact protectors.

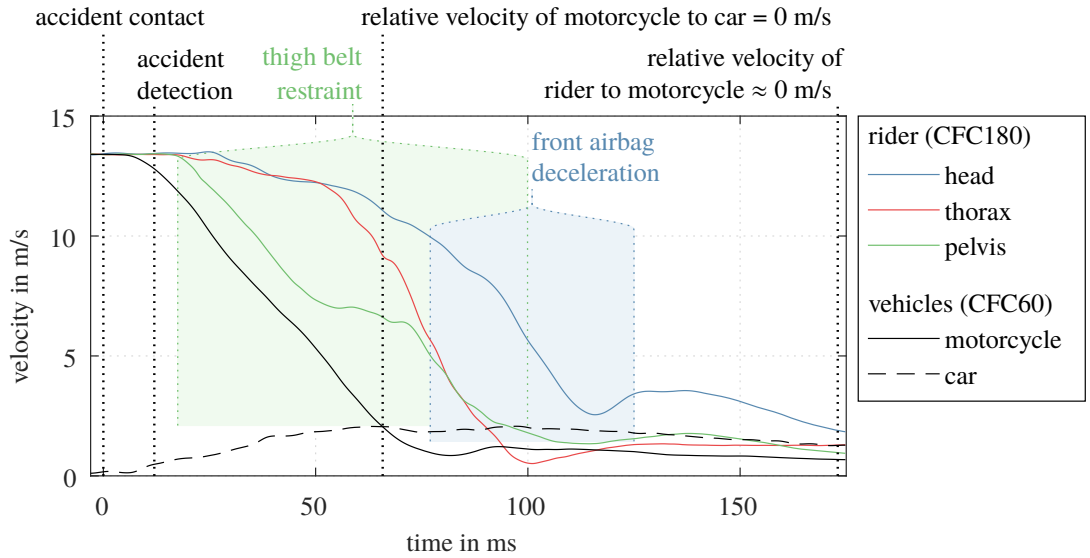

Figure 13: **Velocities of motorcycle with restraint safety systems and motorcyclist's main body parts in a frontal collision according to configuration ⑦ (Full FE simulation shown in Figure 9).**

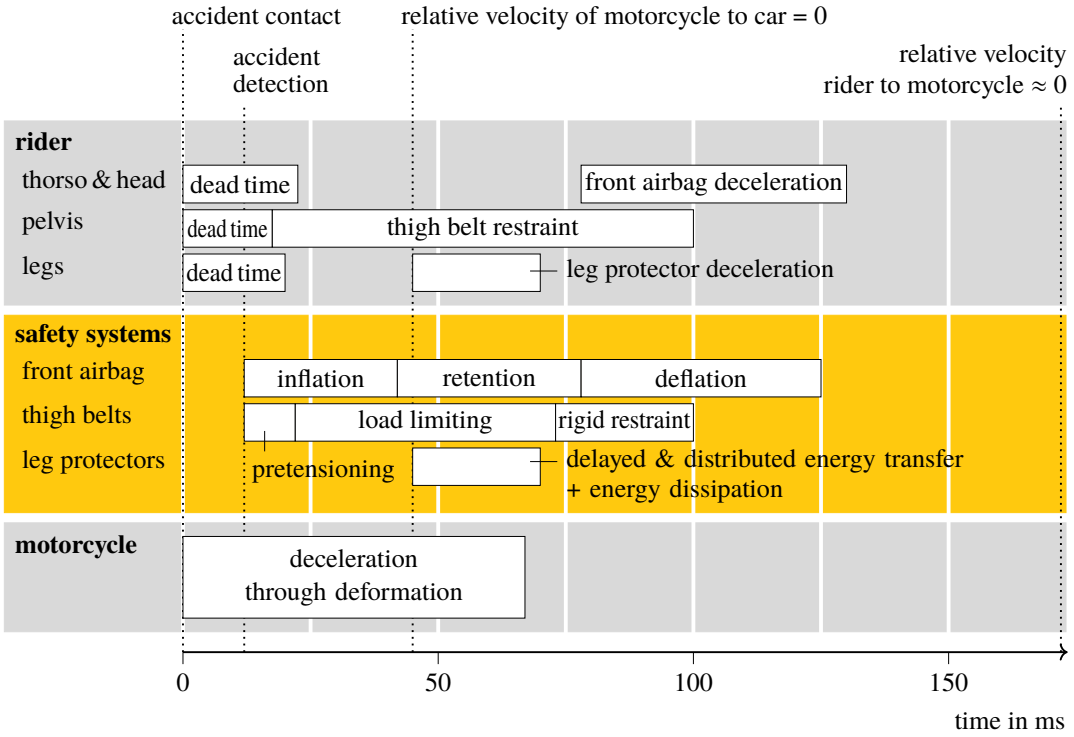

Figure 14: **Schematic chronology of motorcycle with restraint safety systems and rider behaviour in a frontal collision according to configuration ⑦ (Full FE simulation of Figure 9).**

Figure 15 is a comparison of the resulting injury criteria of the conventional motorcycle vs. the motorcycle with the rider restraint. The crash test criteria of the conventional motorcycle are based on the experimental sensor data of the laboratory test; for the motorcycle with rider restraint, they are from the full FE simulation. Change for the better or the worse is highlighted by green and red arrows. Overall, the number of critical values is reduced. Whereby with the current parameters fot the design varibles lead safety-concept related to higher loads for neck axial tension and pelvis and thorax acceleration.

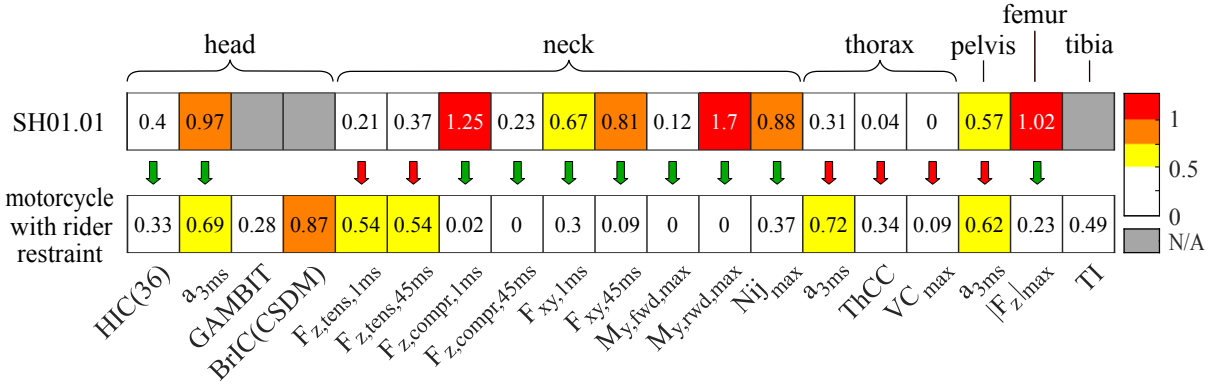

Figure 15: **Injury criteria relative to respective biomechanical limit for conventional motorcycle (top; experimental data of SH01.01) and motorcycle with rider restraint (bottom; full FE simulation).**

DISCUSSION

The work investigates the primary impact behavior of a recommended set of impact scenarios involving PTWs. The motorcycle's safety concept enables a guided rider trajectory and controlled energy dissipation through rider restraint with continuous deceleration during a motorcycle-to-car impact. With few exceptions, recommended injury criteria and respective biomechanical limits indicate tolerable rider loading. Some values for BrIC, TI, and thorax $a_{3\text{ms}}$ are not within the recommended biomechanical limits. A comparison with a conventional motorcycle shows the advantages of controlled and continuous load application onto the body of the rider. The consequences of an accident depend less on the randomness and unpredictability of a conventional accident with multiple possible trajectories than on the design variables of the safety system.

The secondary impact behavior, impacts against other accident opponents, e.g., roadside barriers, and solo accident behavior, have not yet been considered. These types have prevalently long accident histories. The use of full FE models with long computation times is challenging since they are computationally costly, even when complex structural interactions with large deformations occur less in such secondary accident phases and solo accidents. Here, future use of hybrid variants that combine the structural impact response of a full FE model and the large rigid body motions of an MB model seems particularly desirable.

CONCLUSIONS

This work contains

- a virtual prediction of the accident behavior of a motorcycle with passive safety systems,
- a meaningful graphical description of the functional and causal principles of a PTW rider restraint,
- and a quantified performance evaluation of the concept.

Comparable to passive safety for car occupants, a combination of several passive safety systems has shown to be promising in positively influencing the accident behavior and consequences of PTW riders.

REFERENCES

[1] Yperman, I. (2011). Commuting by Motorcycle: Impact Analysis, Report No. 10.69. Transport & Mobility Leuven, Leuven, Belgium.

[2] Brunner, H., Hirz, M., Hirschberg, W., and Fallast, K. (2018). Evaluation of various means of transport for urban areas. Energy, Sustainability and Society, 8:117–121.

[3] Savage, I. (2013). Comparing the fatality risks in united states transportation across modes and over time. Research in Transportation Economics, 43(1):9–22. The Economics of Transportation Safety.

[4] Langwieder, K., Sporner, A., and Polauke, J. (1987). Stand der passiven Sicherheit für den Motorradfahrer und mögliche Entwicklungstendenzen (in German). In Gesellschaft Fahrzeugtechnik, Aktive und passive Sicherheit von Krafträdern: Tagung, Berlin, 8. u. 9. Oktober 1987, VDI-Berichte 657, pages 29–52, Düsseldorf. VDI-Verlag.

[5] Kobayashi, Y. and Makabe, T. (2013). Crash detection method for motorcycle airbag system with sensors on the front fork. In Proceedings of the 23rd International Technical Conference on the Enhanced Safety of Vehicles (ESV), number 13-0344, Seoul, Korea.

[6] Kuroe, T., Namiki, H., and Iijima, S. (2005). Exploratory study of an airbag concept for a large touring motorcycle: Further research second report. In Proceedings of the 19th International Technical Conference on the Enhanced Safety of Vehicles (ESV), number 05-0316, Washington, DC, USA.

[7] Namiki, H., Nakamura, T., and Iijima, S. (2005). A computer simulation for motorcycle rider injury evaluation in collision. In Proceedings of the 19th International Technical Conference on the Enhanced Safety of Vehicles (ESV), number 05-0309, Washington, DC, USA.

[8] Kalliske, I. and Albus, C. (1998). Safety potential of future two-wheel concepts – a challenge. In Proceedings of the 16th International Technical Conference on the Enhanced Safety of Vehicles (ESV), number 98-S10-O-15, pages 2279–92, Winsor Ontario, Canada.

[9] Osendorfer, H. and Rauscher, S. (2001). The development of a new class of two-wheeler vehicles. In Proceedings of the 17th International Technical Conference on the Enhanced Safety of Vehicles (ESV), number 01-S8-O-475, Amsterdam, Netherlands.

[10] Berg, F. A., Bürkle, H., and Schmidts, F. (1998). Analysis of the passive safety of motorcycles using accident investigations and crash tests. In Proceedings of the 16th International Technical Conference on the Enhanced Safety of Vehicles (ESV), number 98-S10-O-11, pages 2221–2236, Winsor Ontario, Canada.

[11] Lindenmann, M., Grandel, J., and Berg, F. (1986). Collision dynamics in experimental simulations of 90° motorcycle collisions against the side of moving passenger cars. In Proceedings of the IRCOBI Conference, pages 289–302, Zurich, Switzerland.

[12] Grandel, J. and Schapter, D. (1987). Investigation into motorcycle, driver and passenger safety in motorcycle accidents with two motorcycle riders. In Proceedings of the 11th International Technical Conference on the Experimental Safety of Vehicles (ESV), pages 888–900, Washington, DC, USA.

[13] Appel, H., Otte, D., and Wüstemann, J. (1986). Epidemiologie von Unfällen motorisierter Zweiradfahrer in der Bundesrepublik Deutschland - Sicherheitsaspekte (in German). In Koch, H., Der Motorradunfall: Beschreibung, Analyse, Prävention, Forschungshefte Zweiradsicherheit, pages 47–92, Bremerhaven. Wirtschaftsverlag NW.

[14] Maier, S., Doléac, L., Hertneck, H., Stahlschmidt, S., and Fehr, J. (2020). Evaluation of a novel passive safety concept for motorcycles with combined multi-body and finite element simulations. In Proceedings of the IRCOBI Conference, number IRC-20-38, pages 250–265, Munich, Germany.

[15] Maier, S., Doléac, L., Hertneck, H., Stahlschmidt, S., and Fehr, J. (2021). Finite element simulations of motorcyclist interaction with a novel passive safety concept for motorcycles. In Proceedings of the IRCOBI Conference, number IRC-21-17, pages 60–78, Munich, Germany.

[16] Maier, S., Helbig, M., Hertneck, H., and Fehr, J. (2021). Characterisation of an energy absorbing foam for motorcycle rider protection in LS-DYNA. In Proceedings of the 13th European LS-DYNA Users Conference, Ulm, Germany. DYNAmore GmbH.

[17] Maier, S., Kempter, F., Kronwitter, S., and Fehr, J. (2022). Positioning and simulation of human body models on a motorcycle with a novel restraint system. In Proceedings of the IRCOBI Conference, number IRC-22-22, pages 82–96, Porto, Portugal.

[18] Barbani, D., Baldanzini, N., and Pierini, M. (2014). Development and validation of an FE model for motorcycle–car crash test simulations. International Journal of Crashworthiness, 19(3):244–263.

[19] Schulz, N., Silvestri Dobrovolny, C., and Hurlebaus, S. (2016). Development of a finite element model of a motorcycle. In Proceedings of the 14th International LS-DYNA Users Conference, Detroit, MI, USA.

[20] Mongiardini, M., Walton, B., Grzebieta, R. H., McKay, M., Menictas, C., Berg, A., and Rücker, P. (2017). Development of a motorcycle FE model for simulating impacts into roadside safety barriers. In Proceedings of the First International Roadside Safety Conference, number E-C220, pages 657–673, San Francisco, CA, USA.

[21] ISO 13232-2:2005 (2005). Motorcycles – Test and Analysis Procedures for Research Evaluation of Rider Crash Protective Devices Fitted to Motorcycles – Part 2: Definition of Impact Conditions in Relation to Accident Data. International Organization for Standardization, Geneva, Switzerland.

[22] Marzougui, D., Samaha, R. R., Cui, C., and Kan, C.-D. S. (2012). Extended validation of the finite element model for the 2001 Ford Taurus passenger sedan. Technical Report NCAC 2012-W-004, The National Crash Analysis Center, The George Washington University, Ashburn, USA.

[23] NHTSA (2012). Mass Reduction for Light-Duty Vehicles for Model Years 2017–2025, Final Report, Report No. DOT HS 811 666. National Highway Transport Safety Association (NHTSA), Washington, DC, USA.

[24] ISO 13232-6:2005 (2005). Motorcycles – Test and Analysis Procedures for Research Evaluation of Rider Crash Protective Devices Fitted to Motorcycles – Part 6: Full-scale Impact-test Procedures. International Organization for Standardization, Geneva, Switzerland.

[25] Berg, F. A., Rücker, P., Bürkle, H., Mattern, R., and Kallieris, D. (2004). Prüfverfahren für die passive Sicherheit motorisierter Zweiräder: Bericht zum Forschungsprojekt FE 82.121/1997 (in German). Berichte der Bundesanstalt für Straßenwesen. F, Fahrzeugtechnik; 49. Wirtschaftsverlag NW, Verlag für neue Wissenschaft, Bremerhaven.

[26] ISO 13232-5:2005 (2005). Motorcycles – Test and Analysis Procedures for Research Evaluation of Rider Crash Protective Devices Fitted to Motorcycles – Part 5: Injury Indices and Risk/Benefit Analysis. International Organization for Standardization, Geneva, Switzerland.

[27] UNECE (2012). Regulation No 94 of the Economic Commission for Europe of the United Nations (UN/ECE) – Uniform Provisions Concerning the Approval of Vehicles with Regard to the Protection of the Occupants in the Event of a Frontal Collision. United Nations Economic Commission for Europe (UNECE), Geneva, Switzerland.

[28] Kleinberger, M., Sun, E., Eppinger, R., Kuppa, S., and Saul, R. (1998). Development of Improved Injury Criteria for the Assessment of Advanced Automotive Restraint Systems, NHTSA Docket No. 98-4405-9. National Highway Transport Safety Association (NHTSA), Washington, DC, USA.

[29] NHTSA (2011). 49 CFR, Section 571.208 – Standard No. 208; Occupant Crash Protection. National Highway Transport Safety Association (NHTSA), Washington, DC, USA.

[30] Newman, J. A. (1986). A Generalized Acceleration Model for Brain Injury Threshold (GAMBIT). In Proceedings of the IRCOBI Conference, pages 121–131, Zurich, Switzerland.

[31] Takhounts, E., Craig, M., Moorhouse, K., McFadden, J., and Hasija, V. (2013). Development of Brain Injury Criteria (BrIC). Stapp Car Crash Journal, 57:243–266.

[32] Melvin, J. W. (1985). The Engineering Design, Development, Testing, and Evaluation Of an Advanced Anthropomorphic Test Device, Phase 1: Concept Definition, Report to Contract No. DTNH22-83-C-07005. National Highway Transport Safety Association (NHTSA), Washington, DC, USA.

[33] Eppinger, R., Sun, E., Bandak, F., Haffner, M., Khaewpong, N., Maltese, M., Kuppa, S., Nguyen, T., Takhounts, E., Tannous, R., Zhang, A., and Saul, R. (1999). Development of Improved Injury Criteria for the Assessment of Advanced Automotive Restraint Systems – II, NHTSA Docket No. 99-6407-5. National Highway Transport Safety Association (NHTSA), Washington, DC, USA.

[34] Lau, I. V. and Viano, D. C. (1986). The viscous criterion – bases and applications of an injury severity index for soft tissues. SAE Transactions, 95:672–691.

[35] Mertz, H. J. (1993). Antropometric test devices. In Nahum, A. M. and Melvin, J. W., Accidental Injury: Biomechanics and Prevention, pages 66–84, New York, NY, USA. Springer New York.

[36] SAE J211-1:1995 (1995). Instrumentation for Impact Test – Part 1 – Electronic Instrumentation. SAE International, Warrendale, PA, USA.